J Biomol NMR (2013) 56:291–301
DOI 10.1007/s10858-013-9761-7

COMMUNICATION

Efficient protocol for backbone and side-chain assignments of large, intrinsically disordered proteins: transient secondary structure analysis of 49.2 kDa microtubule associated protein 2c

Jiří Nováček · Lubomír Janda · Radka Dopitová · Lukáš Žídek · Vladimír Sklenář

Received: 8 April 2013 / Accepted: 7 July 2013 / Published online: 23 July 2013

Abstract Microtubule-associated proteins (MAPs) are abundantly present in axons and dendrites, and have been shown to play crucial role during the neuronal morphogenesis. The period of main dendritic outgrowth and synaptogenesis coincides with high expression levels of one of MAPs, the MAP2c, in rats. The MAP2c is a 49.2 kDa intrinsically disordered protein. To achieve an atomic resolution characterization of such a large protein, we have developed a protocol based on the acquisition of two five-dimensional ^{13}C-directly detected NMR experiments. Our previously published 5D CACONCACO experiment (Nováček et al. in J Biomol NMR 50(1):1–11, 2011) provides the sequential assignment of the backbone resonances, which is not interrupted by the presence of the proline residues in the amino acid sequence. A novel 5D HC(CC-TOCSY)CACON experiment facilitates the assignment of the aliphatic side chain resonances. To streamline the data analysis, we have developed a semi-automated procedure for signal assignments. The obtained data provides the first atomic resolution insight into the conformational state of MAP2c and constitutes a model for further functional studies of MAPs.

Keywords Nuclear magnetic resonance · Intrinsically disordered proteins · Microtubule-associated protein · Transient secondary structure · ^{13}C detection

Introduction

Microtubule-associated proteins (MAPs) play a crucial role in microtubule assembly, stability and dynamics, the process of a fundamental importance in a variety of cellular processes (Gamblin et al. 1996; Drewes et al. 1998; Dehmelt et al. 2003; Roger et al. 2004). The neuronal MAP2 and tau proteins have attracted prominent attention among the MAPs due to the aggregation of tau to Alzheimer paired helical filaments. In contrast to tau, which is mainly present in axons, MAP2 is localized in the dendrites of the neuronal cells (Jalava et al. 2007). MAP2 comprises several proteins, which are transcribed from a single gene through alternative RNA splicing (Doll et al. 1993; Kalcheva et al. 1995). In rodents, that are being extensively studied due to the high similarity with the human genome and a possibility to perform experiments on an animal model, four major MAP2 isoforms are distinguished, which can be divided according to the molecular weight or developmentally regulated expression levels (Kalcheva et al. 1995; Jalava et al. 2007). The low molecular weight MAP2c and MAP2d contain 467 and 498 amino acids, respectively, whereas the high molecular weight MAP2a and MAP2b consist of 1,830 amino acids (Doll et al. 1993; Wille et al. 1992). All four isoforms are similar in the amino acid composition of both carboxy and amino terminal domains. The large difference in size of the high molecular weight isoforms MAP2a and MAP2b is due to a large arm inserted between the N-terminal and C-terminal domains (*vide supra*), which projects the amino terminus

Electronic supplementary material The online version of this article (doi:10.1007/s10858-013-9761-7) contains supplementary material, which is available to authorized users.

J. Nováček · L. Janda · R. Dopitová · L. Žídek (✉) · V. Sklenář
Faculty of Science, NCBR, and CEITEC, Masaryk University, Kamenice 5, 625 00 Brno, Czech Republic
e-mail: lzidek@chemi.muni.cz

further from the microtubule surface (Wille et al. 1992). Therefore, MAP2c represents the smallest fully functional unit for description of MAP2 functions in cellular processes which comprise the interactions of amino or carboxy ends of MAP2 proteins.

MAPs belong to the group of intrinsically disordered proteins (IDPs), whose polypeptide chains exist and function in multiple, quickly inter-converting conformations (Dunker et al. 2000, 2008; Dyson and Wright 2005; Tompa 2005; Fink 2005). The intrinsic disorder predetermines the choice of experimental techniques suitable for structural characterization of MAPs. NMR is the only biophysical technique providing information at the atomic resolution and reporting both on local conformation and long-range contacts (Fink 2005; Dyson and Wright 2005). The high flexibility of the disordered polypeptide chain results in relatively intense and sharp signals in the NMR spectra. Adversely, conformational averaging of the IDPs along with the presence of repetitive motifs in the amino acid sequence cause a severe peak overlap that complicates the analysis of NMR spectra (Motáčková et al. 2010) and represents a major factor limiting the size of the IDPs amenable to NMR studies. As relatively long spin–spin relaxation times would in principle allow to study IDP of an arbitrary size, it is highly desirable to develop methodologies maximizing the attainable resolution.

Various strategies have been applied for chemical shift assignment of IDPs. The standard methodology, based on acquisition of ^{1}H or ^{13}C-detected triple resonance experiments (Grzesiek and Bax 1992; Sattler et al. 1999; Panchal et al. 2001; Rovnyak et al. 2004; Sun et al. 2005; Frueh et al. 2006; Bermel et al. 2006a, 2009b), originally developed for the studies well structured or deuterated proteins, has been employed successfully in a number of studies (Peti et al. 2001; Yao et al. 2001; Bermel et al. 2006b, 2009a; Pannetier et al. 2007; Mukrasch et al. 2009; Motáčková et al. 2009). Recent advances in development of the techniques for processing of reduced dimensionality (Bodenhausen and Ernst 1981, 1982; Szyperski et al. 1993; Ding and Gronenborn 2002; Kim and Szyperski 2003; Kupče and Freeman 2003; Hiller et al. 2005) and randomly sampled data (Barna et al. 1987; Barna and Laue 1987; Schmieder et al. 1994; Orekhov et al. 2001; Stern et al. 2002; Malmodin and Billeter 2005; Marsh et al. 2006; Kazimierczuk et al. 2006; Coggins and Zhou 2007; Kazimierczuk and Orekhov 2011; Hyberts et al. 2012) stimulated design of novel pulse sequences, which allow to correlate sufficient number of atoms for sequential assignment in a single high dimensional experiment (Hiller et al. 2007; Narayanan et al. 2010; Motáčková et al. 2010; Wen et al. 2011; Nováček et al. 2011, 2012; Zawadzka-Kazimierczuk et al. 2012). The groups of Griesinger and Zweckstetter have shown a breakthrough application of both approaches to the assignment of a 441 amino acid long, intrinsically disordered human tau protein (Mukrasch et al. 2009; Narayanan et al. 2010).

Herein, we present an efficient protocol for the assignment of NMR signals in large IDPs based on acquisition of high-dimensional NMR experiments in combination with non-uniform sampling and an appropriate data processing. In addition, we report the assessment of the transient secondary structure motifs present along the MAP2c sequence that is derived from the analysis of assigned chemical shifts. The chemical shift assignment was based on the acquisition of two five-dimensional ^{13}C detected spectra, which provide both the sequential (5D CACONCACO) and side chain (5D HC(CC-TOCSY)CACON) assignments. This approach allowed us to assign backbone atoms of all residues including prolines and 98.2 % ^{1}H and ^{13}C nuclei in aliphatic side chains of the archetypal MAP2c isoform. Our data form a cornerstone for further detailed description of interactions and post-translational modifications underwent by MAP2c in the neurons.

Materials and methods

Sample preparation

The rat brain MAP2c cDNA inserted into the pET3a expression vector, kindly provided by Prof. G. Wiche, was cloned into BL21(DE3)$_{RIL}$ cells. The cells were grown in three litres of ^{13}C, ^{15}N enriched M9 medium to the $OD_{600} \sim 0.7$. Then, the protein expression was induced by 0.4 mM IPTG and the cells were grown for additional 14 h. The thermally stable MAP2c was purified as described earlier (Gamblin et al. 1996). The extract containing the MAP2c protein was mixed with five volumes of 50 mM sodium acetate (pH 5.5), 1 mM EGTA, 1 mM $MgCl_2$, 4 mM β-mercaptoethanol and loaded onto the 6 ml Resource S cation exchange column. Gradient of 0–2 M NaCl in the same buffer was used to elute the protein from the column. Finally, the MAP2c protein was loaded onto the Superdex 75 column. The final sample used for the NMR measurements consisted of 1.2 mM [^{13}C, ^{15}N] MAP2c in 50 mM MOPS (pH 6.9), 100 mM NaCl, 0.7 mM TCEP and 10 % D_2O. The mass spectrometry analysis of the unlabeled sample revealed that the N-terminal methionine residue had been cleaved during the expression.

NMR experiments and data handling

The 5D CACONCACO experiment was measured with the spectral widths set to $7000(aq) \times 4000(^{13}C^{\alpha}) \times 2500(^{15}N) \times 2000(^{13}C') \times 4000(^{13}C^{\alpha})$ Hz. The maximal acquisition

times in the indirectly detected dimensions were set to 26 ms for the $^{13}C^{\alpha}$ dimensions, to 46 ms for the ^{15}N dimension and to 28 ms for the $^{13}C'$ dimension. The data was collected with 8 scans per FID and an interscan delay of 0.3 s. The overall number of 512 complex points was recorded in the acquisition dimension and the overall number of 1,600 hypercomplex points has been randomly distributed (*vide infra*) over the indirectly detected dimensions. The experiment was acquired in 53 h, which is 0.0023 % of the time needed for acquisition of linearly sampled experiment providing similar resolution. The auxiliary 3D (CACO)NCACO experiment was acquired with the spectral widths set to 7000 (aq) × 2500 (^{15}N) × 4000 ($^{13}C^{\alpha}$) Hz. The maximal evolution times in the indirectly detected dimensions were set to 46 ms for the ^{15}N dimension and to 26 ms for the $^{13}C^{\alpha}$ dimension. The data was recorded with 8 scans per FID and a single scan recycle delay of 0.3 s. 512 complex points was acquired in the directly detected dimension and 900 hypercomplex points were detected in indirect dimensions. The 5D HC(CC-TOCSY)CACON (Fig. 2) experiment was measured with the spectral widths set to 7000 (aq) × 2500 (^{15}N) × 4000 ($^{13}C^{\alpha}$) × 12500 ($^{13}C^{ali}$) × 8000 ($^{1}H^{ali}$) Hz. The maximal evolution times in the indirectly detected dimensions were set to 46 ms for the ^{15}N dimension, to 26 ms for the $^{13}C^{\alpha}$ dimension, to 8 ms for the $^{13}C^{ali}$ dimension and to 10 ms for the $^{1}H^{ali}$ dimension. The data was acquired with 6 scans per FID (2 scans per mixing time, mixing times—14.1, 18.8 and 28.3 ms) and an interscan delay of 1.0 s. The overall number of 512 complex points was recorded in the acquisition dimension and the total number of 1,500 hypercomplex points has been randomly distributed over the indirectly detected dimensions. The data was acquired within 71 h which is 0.0016 % of the time needed for acquisition of a linearly sampled experiment with similar resolution. The auxiliary 3D (HC(CC-TOCSY))CACON experiment was acquired with spectral widths set to 7000 (aq) × 2500 (^{15}N) × 4000 ($^{13}C^{\alpha}$) and maximal acquisition times of 46 ms for ^{15}N and 26 ms for $^{13}C^{\alpha}$ indirectly detected dimensions. The data was recorded with 6 scans per FID and a single scan recycle delay of 1.0 s. 512 complex points was recorded in the acquisition dimension and 1,000 hypercomplex points were randomly distributed in the indirect dimensions. All the data was acquired on a 700 MHz Bruker Avance III spectrometer equipped with the $^{1}H/^{13}C/^{15}N$ TXO cryogenic probehead with the z-axis gradients at 27°C.

The non-uniform sampling of the indirectly detected dimensions was utilized for the data acquisition. Poisson disc algorithm (Kazimierczuk et al. 2008) was employed to generate the sampling schedule. This algorithm contains a criterion that defines minimal distances between the generated time points. The off-grid sampling scheme was generated for acquisition of the five-dimensional experiment, whereas the time points were placed on the Cartesian grid in the case of 3D experiments. Multidimensional Fourier transform supplemented with protocol for iterative artifact suppression (Stanek and Koźmiński 2010) was applied to obtain 3D (CACO)NCACO and 3D (HC(CC-TOCSY))CACON spectra. The sparse multidimensional Fourier transform (Kazimierczuk et al. 2009) has been employed to process the 5D CACONCACO and HC(CC-TOCSY)CACON data (both programs are available at http://nmr.cent3.uw.edu.pl/). All the spectra were analyzed in a graphical NMR assignment and integration software Sparky 3.115 (T.D. Goddard and D. G. Kneller, University of California, San Francisco, USA).

The analysis of the transient secondary structure motifs was performed using the SSP (Marsh et al. 2006) and δ2D (Camilloni et al. 2012) programs. A neighbor corrected random coil chemical shifts (Tamiola et al. 2010) were used as a reference values in the SSP program. The observed $H^{\alpha}, C^{\alpha}, C^{\beta}, C'$, and N chemical shifts of MAP2c were used in the SSP analysis, which provided propensities for helical and extended secondary structure motifs. The same set of MAP2c chemical shifts and the internal database of reference chemical shift values was used in the analysis by δ2D program, which further provides the transient population for poly proline II structures.

Results

The chemical shift assignment of MAP2c was performed using two five-dimensional, ^{13}C-directly detected NMR experiments. The sequential assignment of MAP2c was obtained by employing the 5D CACONCACO experiment (Fig. 1a) developed previously in our laboratory (Nováček et al. 2011). Each observed NMR signal in the spectrum encodes the resonance frequencies of five consecutive atoms along the polypeptide backbone (C^{α} and C' of the $(i-1)$th amino acid and N, C^{α} and C' of the ith amino acid). The non-uniform sampling facilitated measurements utilizing long acquisition times in all indirectly detected dimensions which resulted in signals with the line width close to the values determined by the inherent R_2 relaxation rates. As the $^{1}H^{N}$ polarization is not included in the magnetization transfer, the sequential assignment, encoded in the C^{α} and C' chemical shifts, was not interrupted by the presence of the proline residues in the sequence.

In order to assign MAP2c aliphatic side chain resonances, we have designed a new 5D HC(CC-TOCSY) CACON experiment (Fig. 2). The exploited coherence transfer pathway is indicated in Fig. 1b. H^{ali}, C^{ali} chemical

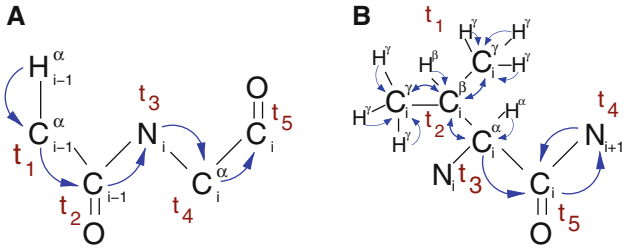

Fig. 1 The transfer of magnetization within the 5D CACONCACO (**a**) and 5D HC(CC-TOCSY)CACON (**b**) experiments. The *blue arrows* indicate individual coherence transfer steps

shifts of the *i*th amino acid are correlated to the C^{α}, C' of the (*i*)th and N of the $(i + 1)$th amino acid of the polypeptide backbone. This experiment is an extension of the previously proposed 3D CCCON and 4D HCCCON correlation schemes (Bermel et al. 2006a, 2012) to five dimensions. The extension of the dimensionality, however, was crucial due to the severe overlap in the 2D CON spectrum of MAP2c (Fig. 3d). The additional dimension extremely simplified the spectra and opened the way for automation of spectra analysis (*vide infra*). The amplitude of the magnetization transfer from C^{ali} to C^{α} exhibits an exponentially decaying periodic dependence on the length of the applied spin-lock and on the configuration of the amino acid side chain. Therefore, the 5D HC(CC-TOCSY)CACON pulse scheme combines three measurements using mixing times of 14.1, 18.8 and 28.3 ms. The data collected in an interleaved manner with 2 scans per mixing time are combined into a single spectrum. This approach ensures a non-zero amplitude of the overall magnetization transfer for all $C^{ali} - C^{\alpha}$ correlations.

Previously, we have applied a manual analysis of the 2D cross-sections extracted from the 5D data using the SMFT algorithm (Kazimierczuk et al. 2009) that allows for checking the signal quality directly in the spectra (Nováček et al. 2011). This is particularly important in the case of a severe peak overlap, when peaks partially overlapping even in the 5D correlation have to be distinguished. However, such an approach requires a considerable amount of time when an IDP as large as 466 amino acids is studied. To overcome this obstacle, we have developed a procedure to automate the process of peak picking and assignments of 5D spectra, while still keeping the possibility to visually check and correct the errors made in the process of the automated peak picking. The analysis of both 5D CACONCACO and 5D HC(CC-TOCSY)CACON spectra requires a list of peak coordinates identified in the auxiliary 3D (CACO)NCACO and 3D (HC(CC-TOCSY))CACON spectra, respectively, and a set of 2D cross-sections from the 5D data sets calculated for the signals identified in the 3D spectra (Kazimierczuk et al. 2010; Nováček et al. 2011). In the case of the 5D CACONCACO data, the algorithm performs the peak picking in the 2D cross-sections, which is tedious to do manually, and generates the list of 5D resonances. The procedure employed to find signals in a cross-section of 5D CACONCACO consists of the following steps: (1) the signal-to-noise (S/N) level in the cross sections is estimated; (2) all peaks with $S/N > 3.0$ are picked; (3) the characteristics (mean and standard deviation) of the peak intensity distribution are calculated with the assumption of the normal distribution of the values; (4) the peaks with intensities deviating from the determined normal distribution at the confidence level of $\alpha = 2.5\ \%$ are selected; (5) five-dimensional peak list of the selected resonances is generated which can be then subjected to automated sequential assignment using one of the well established programs (*vide infra*, Supporting Information S1) or used for manual search of sequential connectivities; (6) all cross-sections where zero or more than one signals were picked are checked manually, as only one signal is expected in each cross-section. Due to the large amount of residues in the amino acid sequence, the overlap of the signals has been encountered in the auxiliary 3D (CACO)NCACO spectrum. Overall, 28 cross-sections generated after the initial peak picking of the 3D (CACO)NCACO spectrum contained more than one signal. However, thanks to the fact that the position of each peak is encoded in five frequencies of different nuclei, the individual signals were resolved in the cross-sections, and thus, the signals overlapping in the 3D (CACO)NCACO spectrum were identified. The peak picking and assignment of 5D HC(CC-TOCSY)CACON proceeds as follows: (1) sequential assignment information is transferred into the auxiliary 3D (HC(CC-TOCSY))CACON spectrum and a 2D cross-section out of the 5D HC(CC-TOCSY)CACON is calculated for each signal found in the 3D spectrum; (2) iterative peak picking at varying intensity levels (starting from $S/N = 30.0$) is performed in the regions spanning the typical chemical shift values of the individual $^{1}H - ^{13}C$ pairs of the particular amino acid side chain; (3) the iterations are stopped once the expected number of signals is picked or the limit of number of iterations is reached; (4) resulting signals are assigned to the particular spin system; (5) report of all unsuccessfully picked $^{1}H - ^{13}C$ spin pairs is generated. The described procedure has been incorporated into a Python extension for the program Sparky and can be downloaded from http://www.ncbr.muni.cz/sparky_extension/peakPick.tgz.

The 5D CACONCACO spectrum for the sequential assignment of MAP2c was measured within 53 h. The analysis of the data provided an unambiguous sequential assignment for 460 out of the 466 amino acids. The signals of residues S183, K347, C348 and R425 were weak in the auxiliary 3D (CACO)NCACO spectrum and broadened beyond the detection limit in the 5D spectrum. No signals were observed for residues G349 and S426 in the 3D or 5D

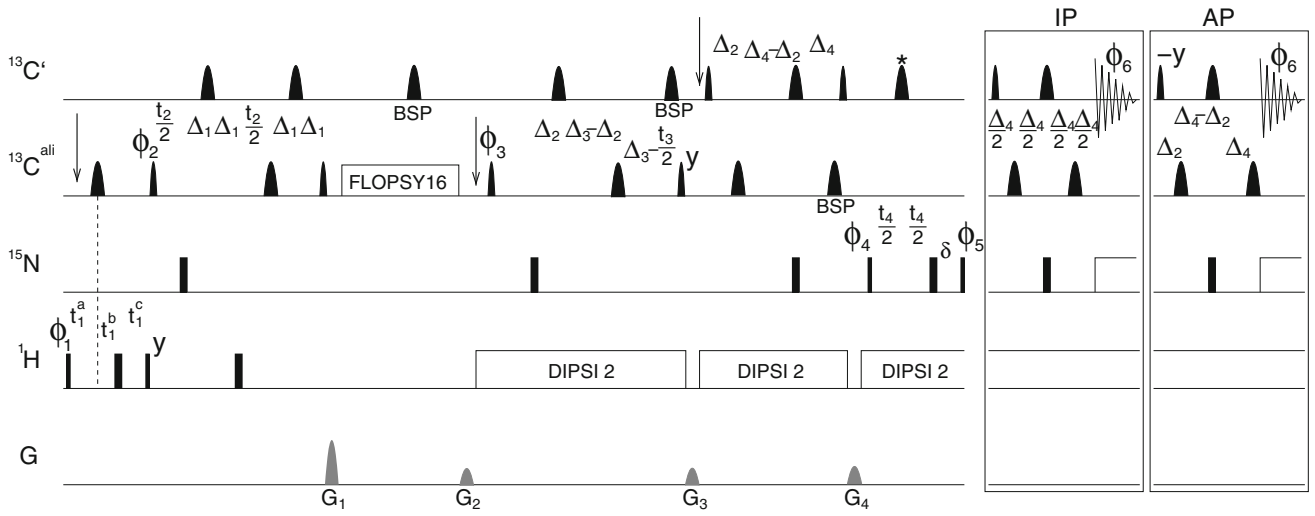

Fig. 2 Pulse sequence scheme of the 5D HC(CC-TOCSY)CACON experiment. The carrier frequencies were placed at the resonance frequency of the water signal for ^{1}H, at 41.0 ppm (*first arrow in line* denoted as $^{13}C^{ali}$) and 55.0 ppm (*second arrow in line* of $^{13}C^{ali}$) for $^{13}C^{ali}$, at 123.5 ppm for ^{15}N, and at 175.0 ppm for $^{13}C'$. The *vertical arrows* indicate the switching of the carrier frequency on the ^{13}C channel. The *narrow and wide rectangular shapes* stand for 90° and 180° high power pulses. The *narrow and wide filled round symbols* represent selective 274 μs 90° Q5 (Emsley and Bodenhausen 1990) (or time-reversed Q5) and 219 μs 180° Q3 (Emsley and Bodenhausen 1990) used for $^{13}C'$ or $^{13}C^{ali}$ excitation resp. inversion on the 700 MHz spectrometer. The ^{13}C *shaped pulse marked with asterisk* represents an 500 μs adiabatic Chirp pulse (Bohlen and Bodenhausen 1993) used for a simultaneous inversion of $^{13}C'$ and $^{13}C^{\alpha}$. BSP denotes pulses for compensation of the off-resonance effects. All the pulses were applied with the *x* phase unless noted differently. TOCSY mixing on $^{13}C^{ali}$ (FLOPSY-16 (Kadkhodaie et al. 1991)), and the decoupling on ^{1}H (DIPSI-2 (Shaka et al. 1988)) and ^{15}N (GARP-4 (Shaka et al. 1985)) are indicated by *white rectangles*. The IPAP acquisition scheme (Ottiger et al. 1998) was implemented to avoid signal splitting in the directly detected dimension due to the $^{13}C^{\alpha}$ –$^{13}C'$ coupling. The *line* denoted with G stands for pulsed field gradients applied along the *z*-axis. The 1,000 μs sine-bell shaped gradients were applied with the following strength: G_1, 36.0 G/cm; G_2, 30.0 G/cm, G_3, 19.4 G/cm; G_4, 6.6 G/cm. The pulses were applied with the following phases: $\phi_1 = x$; $\phi_2 = y, -y$; $\phi_3 = x$; $\phi_4 = 2(x), 2(-x)$; $\phi_5 = 4(x), 4(-x)$; $\phi_6 = x, 2(-x), x, -x, 2(x), -x$. The initial lengths of the delays were: $\Delta_1 = 475\,\mu s, \Delta_2 = 4.5\,ms, \Delta_3 = 13.5\,ms$, $\delta_4 = 506\,\mu s, \Delta_4 = 12.5\,ms, t_1^a = 1.8\,ms, t_1^b = 0.0\,ms, t_1^c = 1.8\,ms$. The evolution of the chemical shift of the $^{1}H^{ali}$ was performed in the semi-constant time manner incrementing t_1^a, t_1^b, t_1^c delays as follows: $\Delta t_1^a = 1/2SW, \Delta t_1^c = -t_1^c(0)/TD, \Delta t_1^b = \Delta t_1^a + \Delta t_1^c$, where SW and TD denote spectral width and number of complex points acquired in the indirect dimension, respectively. The detection of the individual quadrature components of the signal was achieved by incrementation of ϕ_1, ϕ_2, ϕ_3 or ϕ_4 in the States manner

CACONCACO spectrum. The higher sensitivity of the 5D HC(CC-TOCSY)CACON experiment, measured within 71 h, allowed to observe all the signals and proved the assignment of residues S183, K347, C348 and R425. Additionally, signals of G349 and S426 were detected and unambiguously assigned in the 5D HC(CC-TOCSY)CACON spectrum based on knowledge of the nitrogen resonance frequency of subsequent residues S350 and S427, respectively. Out of the 2,094 ^{1}H and 1,392 ^{13}C aliphatic resonances of the 466 amino acid long MAP2c construct, the overall number of 47 ^{1}H and 17 ^{13}C resonance frequencies were not identified in the 5D HC(CC-TOCSY)CACON spectrum. The complete assignment was deposited into the Biological Magnetic Resonance Bank (access code 19135).

Originally, sequential connectivities among the signals identified in the 5D CACONCACO experiment were searched manually. To test the applicability of the 5D CACONCACO data for the automated sequential assignment, we have subjected the list of resonances automatically picked using the described procedure into the program MARS (Jung and Zweckstetter 2004). The final set of all resonances identified in the 3D (CACO)NCACO experiment during the manual assignment was used to generate the 2D cross-sections, which were then automatically peak picked. Only one of the resonances which were repeatedly picked due to the overlap in the 3D (CACO)NCACO spectrum was used when generating the input for the MARS program (Jung and Zweckstetter 2004). As six residues were missing in the spectra and N-terminal residue is not observable in the 5D CACONCACO spectra, the final resonance list contained 459 pseudo residues. The analysis by program MARS (Supporting Information S1) resulted in correct and unambiguous assignment of 412 amino acids. The correct assignment was one of the suggested solutions in the case of further 41 amino acids and only 6 amino acids were assigned incorrectly.

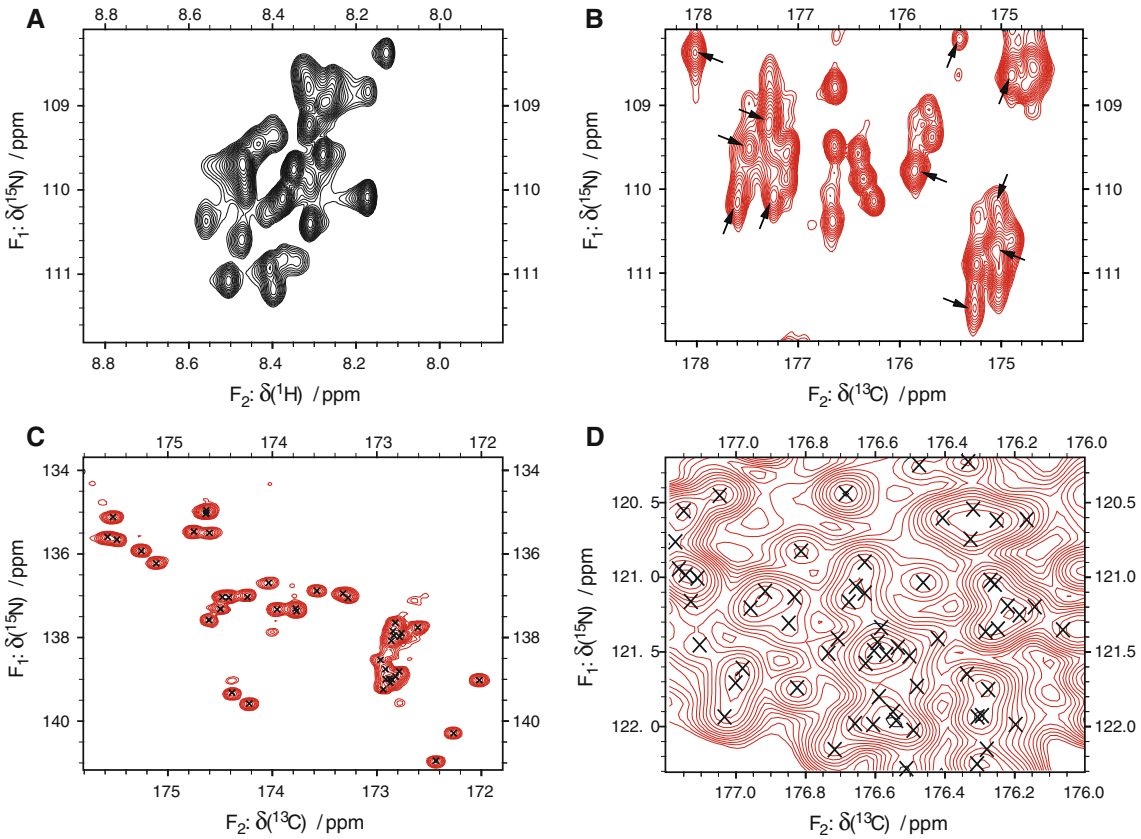

Fig. 3 The region of the glycine signals in the $^{1}H - ^{15}N$ HSQC spectrum (**a**), and the glycine (**b**), proline (**c**), and central (**d**) regions of the ^{13}C-detected 2D CON spectrum. The *arrows* in the **b** (2D CON experiment) indicate peaks broadened beyond the detection limit in the **a** (2*D* $^{1}H - ^{15}N$ HSQC experiment). The chemical shift range in the direct dimensions in **a** and **b** was chosen so that the average line width (defined as FWHH) of ^{1}H (27 Hz) and ^{13}C (20.5 Hz) appears identical in both plots

Discussion

The inherently low sensitivity together with fast relaxation represent two major factors limiting the application of NMR in structural biology of large, well-structured proteins. In contrast, the favorable relaxation properties of IDPs facilitate the application of NMR to investigate long polypeptide chains lacking a well-defined spatial structure. The chemical shift averaging caused by rapidly interconverting conformations of the IDPs results in a high overlap of the peaks in the spectra. Therefore, selection of a correlation scheme, which provides well-resolved signals even for the IDPs with a high degeneracy in the primary structure, is needed. Herein, we document that a combination of two ^{13}C-detected 5D experiments based on CACONCACO and HC(CC-TOCSY)CACON magnetization transfers provides sufficient resolution allowing unambiguous assignment of a 49.2 kDa intrinsically disordered protein MAP2c. ^{13}C direct detection not only improved resolution in the direct dimension with respect to the $^{1}H^{N}$ detection but was particularly important for the assignment of MAP2c, which contains 43 prolines in the sequence (~9 % of all residues, Fig. 3c). Four PGTP, two PPSP and four other PxxP motifs in the MAP2c sequence were assigned unambiguously. Moreover, the sensitivity of the ^{13}C-detected experiments was not compromised by the exchange of $^{1}H^{N}$ with solvent, which is relatively fast in IDPs at near physiological conditions due to the lack of hydrogen bonding. Figure 3 documents that the exchange was significant at the conditions used in our study (pH 6.9, 27 °C). All the signals broadened beyond the detection limit in $^{1}H - ^{15}N$ HSQC spectrum (Fig. 3a) are easily detected in the ^{13}C 2D CON spectrum (Fig. 3b).

The C^{α} and C' chemical shifts obtained in the process of sequential assignment are direct indicators of transient secondary structure, both being more sensitive to the presence of a helical conformation. The acquisition of the 5D HC(CC-TOCSY)CACON spectrum supplied the chemical shifts of signals, which are rather sensitive to an extended conformation (H^{α}, C^{β}) and provided the assignment of the aliphatic side chain resonance frequencies. The cross sections of both 5D CACONCACO (Fig. 4a) and 5D HC(CC-TOCSY)CACON (Fig. 4b) are mostly free of overlap, which predestines them for an automated analysis.

We have designed and applied a semi-automated protocol, which combines the peak picking and resonance assignment, the two most time consuming steps of data analysis, and allows the user to manually add missed peaks or correct miss-assigned signals. The analysis of the TOCSY spectrum is especially suitable for the automation of the peak picking and fast assignment. The whole set of 464 2D cross sections was analyzed within 70 s (on Intel i5 2.4 GHz processor operating at 64 bit). The subsequent manual check revealed that three signals were incorrectly picked and assigned, and the resonance frequencies of 24 $^{1}H - {}^{13}C$ cross peaks were not picked in the automated procedure. In summary, analysis of two five-dimensional and two auxiliary three-dimensional spectra of a single 49.2 kDa protein construct, acquired within 6 days, provided 100 % backbone and 98.2 % aliphatic side chain assignment. A comparison with the current benchmark in the field, the 92 % assignment of 45.7 kDa human tau protein obtained from a combination of one 5D and one 7D experiment (Narayanan et al. 2010) or from three (4,3)D reduced dimensionality experiments (Harbison et al. 2012) proves that our methodology is well suited for an efficient investigation of large IDPs. In addition, our protocol also provides assignments of the aliphatic side chains.

The assigned chemical shifts were used to characterize prevailing transient secondary structure motifs along the MAP2c sequence (Fig. 5). The evaluation was performed based on the calculation of the secondary chemical shifts, direct indicators of secondary structure. Two programs, SSP (Marsh et al. 2006) and δ2D (Camilloni et al. 2012), capable of combining all relevant chemical shifts ($H^{\alpha}, C^{\alpha}, C^{\beta}, C'$, and N in our case) in a single score of transient secondary structure propensity were used. The recently published neighbor corrected random coil chemical shifts (Tamiola et al. 2010), employed as the reference values, improved accuracy of the analysis by the SSP program. The score obtained by the SSP analysis reports on the content of the conformers present in a secondary structure. The values of +1 and −1 are obtained when α or β structure is fully formed, respectively, whereas the value of e.g. 0.4 indicates that 40 % molecules in the ensemble populate α helical structure at the position of the analysed residue (Marsh et al. 2006). The δ2D program provides, besides α-helical and β-strand populations, also the propensity of the poly-proline II (PPII) structure. Four structural elements (α-helix, β-strand, random coil, and poly-proline II) are defined and the predicted values correspond to the probabilities of their occupation for a given residue (Camilloni et al. 2012). The probabilities for a certain structural element higher than 10 % (δ2D score 0.1) are considered significant (M. Vendruscolo, personal communication). In contrast to SSP, the external reference values

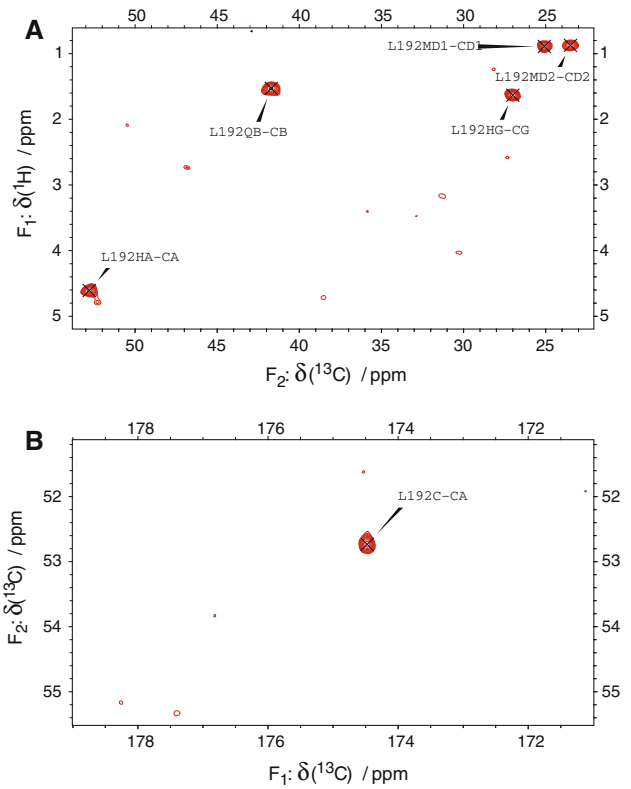

Fig. 4 The 2D cross section calculated from 5D HC(CC-TOCSY)CACON data at the position L192CA-P193N-L192C (**a**), and cross-section calculated from the 5D CACONCACO data at P193N-CA-C (**b**)

cannot be used in the δ2D program. Comparison of the local conformational propensities defined as difference of the $^{13}C^{\alpha}$ and $^{13}C^{\beta}$ secondary chemical shifts with the secondary structure propensities calculated by SSP and δ2D programs showed that δ2D is slightly biased towards the extended (PPII and β-strand) structures. Therefore, we have used SSP as a primary source of the secondary structure propensities and δ2D for differentiation between β-strand and PPII motifs.

MAP2c is a multidomain protein, which is transcribed by alternative RNA splicing from a single gene common for all MAP2 proteins. MAP2c is the smallest of all isoforms and all its domains are present in other isoforms, which makes it a good model system for all MAP2 proteins. The acidic N-terminal domain (residues M1–E151 shown in red in Fig. 6) exhibits the lowest sequence identity to other MAPs (18 % with tau protein). The secondary structure propensity based on the analysis by the program SSP (Fig. 5a) revealed several segments with a helical propensity and one segment (K117–P139) with a relatively high propensity for an extended structure. Strikingly, the two regions with highest helical propensity (A82–V95 and T99–H116) coincide with the binding site

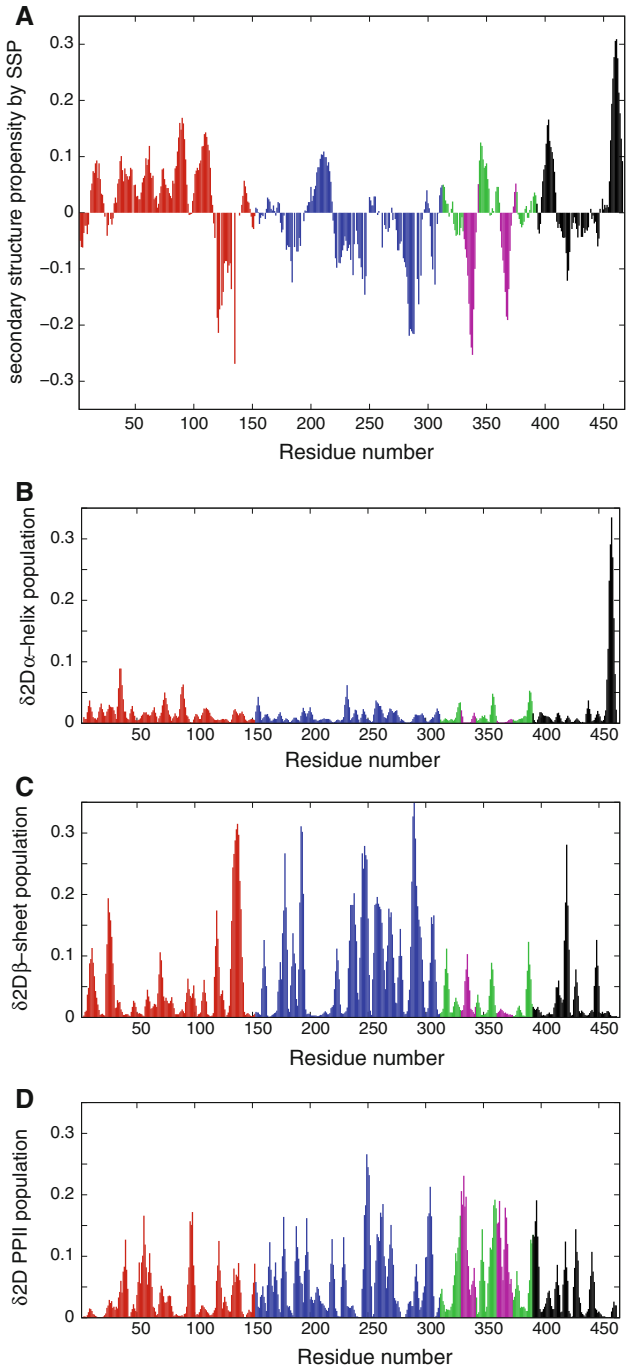

Fig. 5 Transient secondary structure propensities of MAP2c given by SSP algorithm (**a**). Population of the helical (**b**), beta (**c**), and poly proline II (**d**) conformation analysed by δ2D. The *color* coding to individual domains in MAP2c sequence. The positive and negative values in **a** are indicative of helical or extended structure, respectively

for a regulatory subunit (RII) of one of the most abundant neuronal kinases, protein kinase A, localized between R84 and V105 by mutation analysis (Dehmelt et al. 2003). This suggests that the interaction with protein kinase A takes place via a helical interface of MAP2c, which is in

```
MADERKDEGK APHWTSASLT EAAAHPHSPE
MKDQGGSGEG LSRSANGFPY REEEEGAFGE
HGSQGTYSDT KENGINGELT SADRETAEEV
SARIVQVVTA EAVAVLKGEQ EKEAQHKDQP
AALPLAAEET VNLPPSPPPS PASEQTAALE
EATSGESAQA PSAFKQAKDK VTDGITKSPE
KRSSLPRPSS ILPPRRGVSG DREENSFSLN
SSISSARRTT RSEPIRRAGK SGTSTPTTPG
STAITPGTPP SYSSRTPGTP GTPSYPRTPG
TPKSGILVPS EKKVAIIRTP PKSPATPKQL
RLINQPLPDL KNVKSKIGST DNIKYQPKGG
QVQIVTKKID LSHVTSKCGS LKNIRHRPGG
GRVKIESVKL DFKEKAQAKV GSLDNAHHVP
GGGNVKIDSQ KLNFREHAKA RVDHGAEIIT
QSPSRSSVAS PRRLSNVSSS GSINLLESPQ
LATLAEDVTA ALAKQGL
```

Fig. 6 Primary structure of the 467 amino acid long rat brain MAP2c. The N-terminal methionine (*gray*) has been cleaved off by the *E. coli*. The amino terminal acidic domain is colored in *red*, the proline rich domain is depicted in *blue*. MAP2c microtubule binding domain consists of three microtubule binding repeat (*green*) separated by inter-repeats (*magenta*). The C-terminal domain is depicted in *black*

accordance with the NMR structures of two different peptides binding the RII subunit (Newlon et al. 2001). The δ2D analysis identified a tendency to form PPII in the protein kinase A binding site and a β-sheet propensity in the region K117–P139. The proline rich domain of MAP2c (blue in Fig. 6) encompasses several consensus SH3 binding motifs (PxxP) and target sites for proline-directed protein kinases (Lim and Halpain 2000; Zamora-Leon et al. 2001). The SSP analysis (Fig. 5a) shows preferences to form extended conformation except for the region of residues G197–R218. The high content of proline residues implicates possible formation of the PPII structure. However, the δ2D program did not provide clear distinction between propensities for β-strands (Fig. 5c) and PPII (Fig. 5d), whose regions are close in the Ramachandran plot. In any case, both programs showed that the poly proline domain of MAP2c is prevalently extended with respect to α helical structure, which may be important for interactions or posttranslational modifications. The microtubule-binding domain (MTBD) consists of three imperfect microtubule-binding repeats (MTBR, residues V313–G330, V344–G361, A376–G393, green in Fig. 6) separated by two inter-repeat (IR) regions (residues Q331–H343 and R362–K375, magenta in Fig. 6). MTBD is responsible for binding not only to microtubules, but also to actin (Roger et al. 2004), where MAP2c bundles the actin filaments. Both MTBRs and IRs take part in the microtubule binding (Al-Bassam et al. 2002). The chemical shifts show a well localized propensity of the extended structure, which coincides with two inter-repeat regions (Fig. 5a). The δ2D program identifies this regions as PPII structures (Fig. 5d). Further, the helical propensity of the central MTBR indicates that this region might be involved in the initiation of the microtubule binding. This is in accord with the results

of a mutagenetic study showing that the MAP2c mutants containing ontly the central MTBR and the second IR exhibit a microtubule polymerization activity similar to the wild type MAP2c (Ludin et al. 1996). Interestingly, both programs predicted the highest helical propensity (over 30 %) in the region of the C-terminal domain between A455 and L467 (Fig. 5a, b). To our knowledge, there is no specific function currently assigned to this region. The comparison with the available secondary C^{α} chemical shifts for human tau protein (Mukrasch et al. 2009) shows a similar probability for α helical structure in the C-terminal regions. Besides, the trends for extended structure in the IRs are observable in the $^{13}C^{\alpha}$ chemical shifts of tau, although they are not as pronounced as in the study of MAP2c including $^{1}H^{\alpha}$ and $^{13}C^{\beta}$, presented here. In summary, the analysis of the chemical shifts reveals that MAP2c is not completely disordered in the unbound state, but forms transient secondary structure motifs related to its function.

Conclusions

Although MAP2c is a very important neuronal protein, which has been shown to take part in multitude of interactions, the atomic resolution information about MAP2c was still missing. We have undertaken an NMR study to fill this gap and have provided complete backbone and 98.2 % side chain chemical shift assignment of this 49.2 kDa IDP, which can serve as a prototypical system for studies of all MAP2 proteins. Analysis of the obtained chemical shifts identified several well-defined regions of distinct transient secondary structure. These regions nicely correlate with the functional motifs revealed earlier by mutagenesis.

Acknowledgments This work was supported by the Czech Science Foundation, Grant number P206/11/0758 (J.N., L.J. and L.Z.). The partial support by the project "CEITEC - Central European Institute of Technology" from European Regional Development Fund, Grant number CZ.1.05/1.1.00/02.0068, and the Joint Research Activity of the 7th Framework program of the EC (BioNMR n. 261863) is also acknowledged.

References

Al-Bassam J, Ozer RS, Safer D, Halpain S, Milligan RA (2002) MAP2 and tau bind longitudinally along the outer ridges of microtubule protofilaments. J Cell Biol 157(7):1187–1196

Barna J, Laue E (1987) Comparison of conventional and exponential sampling for 2D NMR experiments: application to a 2D NMR spectrum of a protein. J Magn Reson 75:384–389

Barna J, Laue E, Mayger M, Skilling J, Worrall S (1987) Exponential sampling: an alternative method for sampling in two-dimensional NMR experiments. J Magn Reson 73:69–77

Bermel W, Bertini I, Felli IC, Kummerle R, Pierattelli R (2006a) Novel ^{13}C direct detection experiments, including extension to the third dimension, to perform the complete assignment of proteins. J Magn Reson 178(1):56–64

Bermel W, Bertini I, Felli IC, Lee YM, Luchinat C, Pierattelli R (2006b) Protonless NMR experiments for sequence-specific assignment of backbone nuclei in unfolded proteins. J Am Chem Soc 128(12):3918–3919

Bermel W, Bertini I, Csizmok V, Felli IC, Pierattelli R, Tompa P (2009a) H-start for exclusively heteronuclear NMR spectroscopy: the case of intrinsically disordered proteins. J Magn Reson 198(2):275–281

Bermel W, Bertini I, Felli IC, Pierattelli R (2009b) Speeding up ^{13}C direct detection biomolecular NMR spectroscopy. J Am Chem Soc 131(42):15339–15345

Bermel W, Bertini I, Felli IC, Gonnelli L, Koźmiński W, Piai A, Pierattelli R, Stanek J (2012) Speeding up sequence specific assignment of IDPs. J Biomol NMR 53(4):293–301

Bodenhausen G, Ernst R (1981) The accordion experiment, a simple approach to three dimensional NMR spectroscopy. J Magn Reson 45:367–373

Bodenhausen G, Ernst R (1982) Direct determination of rate constants of slow dynamic processes by two-dimensional "accordion" spectroscopy in nuclear magnetic resonance. J Am Chem Soc 104:1304–1309

Bohlen J, Bodenhausen G (1993) Experimental aspects of chirp NMR-spectroscopy. J Magn Reson Ser A 102(3):293–301

Camilloni C, De Simone A, Vranken WF, Vendruscolo M (2012) Determination of secondary structure populations in disordered states of proteins using nuclear magnetic resonance chemical shifts. Biochemistry 51(11):2224–2231

Coggins B, Zhou P (2007) Sampling of the time domain along concentric rings. J Magn Reson 184:207–221

Dehmelt L, Smart FM, Ozer RS, Halpain S (2003) The role of microtubule-associated protein 2c in the reorganization of microtubules and lamellipodia during neurite initiation. J Neurosci 23(29):9479–9490

Ding K, Gronenborn A (2002) Novel 2D triple-resonance NMR experiments for sequential resonance assignments of proteins. J Magn Reson 156:262–268

Doll T, Meichsner M, Riederer BM, Honegger P, Matus A (1993) An isoform of microtubule-associated protein 2 (MAP2) containing four repeats of the tubulin-binding motif. J Cell Sci 106(Pt 2):633–639

Drewes G, Ebneth A, Mandelkow EM (1998) MAPs, MARKs and microtubule dynamics. Trends Biochem Sci 23(8):307–311

Dunker AK, Obradovic Z, Romero P, Garner EC, Brown CJ (2000) Intrinsic protein disorder in complete genomes. Genome Inform Ser Workshop Genome Inform 11:161–171

Dunker AK, Oldfield CJ, Meng J, Romero P, Yang JY, Chen JW, Vacic V, Obradovic Z, Uversky VN (2008) The unfoldomics decade: an update on intrinsically disordered proteins. BMC Genomics 9(Suppl 2):S1

Dyson HJ, Wright PE (2005) Intrinsically unstructured proteins and their functions. Nat Rev Mol Cell Biol 6(3):197–208

Emsley L, Bodenhausen G (1990) Gaussian pulse cascades—new analytical functions for rectangular selective inversion and in-phase excitation in NMR. Chem Phys Lett 165(6):469–476

Fink AL (2005) Natively unfolded proteins. Curr Opin Struct Biol 15(1):35–41

Frueh DP, Sun ZY, Vosburg DA, Walsh CT, Hoch JC, Wagner G (2006) Non-uniformly sampled double-TROSY hNcaNH experiments for NMR sequential assignments of large proteins. J Am Chem Soc 128(17):5757–5763

Gamblin TC, Nachmanoff K, Halpain S, Williams RC (1996) Recombinant microtubule-associated protein 2c reduces the

dynamic instability of individual microtubules. Biochemistry 35(38):12,576–12,586
Grzesiek S, Bax A (1992) Improved 3D triple-resonance NMR techniques applied to a 31-kDa protein. J Magn Reson 96:432–440
Harbison NW, Bhattacharya S, Eliezer D (2012) Assigning backbone NMR resonances for full length tau isoforms: efficient compromise between manual assignments and reduced dimensionality. PLoS One 7(4):e34679
Hiller S, Fiorito F, Wüthrich K, Wider G (2005) Automated projection spectroscopy (APSY). PNAS 102:10876–10881
Hiller S, Wasmer C, Wider G, Wüthrich K (2007) Sequence-specific resonance assignment of soluble nonglobular proteins by 7D APSY-NMR spectroscopy. J Am Chem Soc 129:10823–10828
Hyberts SG, Milbradt AG, Wagner AB, Arthanari H, Wagner G (2012) Application of iterative soft thresholding for fast reconstruction of NMR data non-uniformly sampled with multidimensional Poisson Gap scheduling. J Biomol NMR 52(4):315–327
Jalava NS, Lopez-Picon FR, Kukko-Lukjanov TK, Holopainen IE (2007) Changes in microtubule-associated protein-2 (MAP2) expression during development and after status epilepticus in the immature rat hippocampus. Int J Dev Neurosci 25(2):121–131
Jung YS, Zweckstetter M (2004) Mars—robust automatic backbone assignment of proteins. J Biomol NMR 30(1):11–23
Kadkhodaie M, Rivas O, Tan M, Mohebbi A, Shaka A (1991) Broadband homonuclear cross polarization using flip-flop spectroscopy. J Magn Reson 91(2):437–443
Kalcheva N, Albala J, O'Guin K, Rubino H, Garner C, Shafit-Zagardo B (1995) Genomic structure of human microtubule-associated protein 2 (MAP-2) and characterization of additional MAP-2 isoforms. Proc Natl Acad Sci USA 92(24):10894–10898
Kazimierczuk K, Orekhov VY (2011) Accelerated NMR spectroscopy by using compressed sensing. Angew Chem Int Ed Engl 50(24):5556–5559
Kazimierczuk K, Koźmiński W, Zhukov I (2006) Two-dimensional Fourier transform of arbitrarily sampled NMR data sets. J Magn Reson 179:323–328
Kazimierczuk K, Zawadzka A, Koźmiński W (2008) Optimization of random time domain sampling in multidimensional NMR. J Magn Reson 192:123–130
Kazimierczuk K, Zawadzka A, Koźmiński W (2009) Narrow peaks and high dimensionalities: exploiting the advantages of random sampling. J Magn Reson 205:286–292
Kazimierczuk K, Zawadzka-Kazimierczuk A, Komiski W (2010) Non-uniform frequency domain for optimal exploitation of non-uniform sampling. J Magn Reson 205(2):286–292
Kim S, Szyperski T (2003) GFT NMR, a new approach to rapidly obtain precise high-dimensional NMR spectra information. J Am Chem Soc 125:1385–1393
Kupče E, Freeman R (2003) Projection-reconstruction of three-dimensional NMR spectra. J Am Chem Soc 125:13958–13959
Lim R, Halpain S (2000) Regulated association of microtubule-associated protein 2 (MAP2) with Src and Grb2: evidence for MAP2 as a scaffolding protein. J Biol Chem 275:20578–20587
Ludin B, Ashbridge K, Fünfschilling U, Matus A (1996) Functional analysis of the MAP2 repeat domain. J Cell Sci 109:91–99
Malmodin D, Billeter M (2005) Multiway decomposition of NMR spectra with coupled evolution periods. J Am Chem Soc 127:13486–13487
Marsh JA, Singh VK, Jia Z, Forman-Kay JD (2006) Sensitivity of secondary structure propensities to sequence differences between alpha- and gamma-synuclein: implications for fibrillation. Protein Sci 15(12):2795–2804
Motáčková V, Kubíčková M, Kožíšek M, Šašková K, Švec M, Žídek L, Sklenář V (2009) Backbone ^{1}H, ^{13}C, and ^{15}N NMR assignment for the inactive form of the retroviral protease of the murine intracisternal A-type particle, inMIA-14 PR. Biomol NMR Assign 3:261–264
Motáčková V, Nováček J, Zawadzka-Kazimierczuk A, Kazimierczuk K, Žídek L, Šanderová H, Krásný L, Koźmiński W, Sklenář V (2010) Strategy for complete NMR assignment of disordered proteins with highly repetitive sequences based on resolution-enhanced 5D experiments. J Biomol NMR 48(3):169–177
Mukrasch MD, Bibow S, Korukottu J, Jeganathan S, Biernat J, Griesinger C, Mandelkow E, Zweckstetter M (2009) Structural polymorphism of 441-residue tau at single residue resolution. PLoS Biol 7(2):e34
Narayanan R, Durr U, Bibow S, Biernat J, Mandelkow E, Zweckstetter M (2010) Automatic assignment of the intrinsically disordered protein tau with 441-residues. J Am Chem Soc 132:11906–11907
Newlon MG, Roy M, Morikis D, Carr DW, Westphal R, Scott JD, Jennings PA (2001) A novel mechanism of PKA anchoring revealed by solution structures of anchoring complexes. EMBO J 20(7):1651–1662
Nováček J, Zawadzka-Kazimierczuk A, Papoušková V, Žídek L, Šanderová H, Krásný L, Koźmiński W, Sklenář V (2011) 5D 13C-detected experiments for backbone assignment of unstructured proteins with a very low signal dispersion. J Biomol NMR 50(1):1–11
Nováček J, Haba NY, Chill JH, Žídek L, Sklenář V (2012) 4D non-uniformly sampled HCBCACON and ^{1}J(NCα)-selective HCBCANCO experiments for the sequential assignment and chemical shift analysis of intrinsically disordered proteins. J Biomol NMR 53(2):139–148
Orekhov V, Ibraghimov I, Billeter M (2001) Munin: A new approach to multi-dimensional NMR spectra interpretation. J Biomol NMR 20:49–60
Ottiger M, Delaglio F, Bax A (1998) Measurement of J and dipolar couplings from simplified two-dimensional NMR spectra. J Magn Reson 131(2):373–378
Panchal S, Bhavesh N, Hosur R (2001) Improved 3D triple resonance experiments, HNN and HN(C)N, for HN and 15N sequential correlations in (13C, 15N) labeled proteins: application to unfolded proteins. Journal of Biomolecular NMR 20:135–147
Pannetier N, Houben K, Blanchard L, Marion D (2007) Optimized 3D-NMR sampling for resonance assignment of partially unfolded proteins. J Magn Reson 186(1):142–149
Peti W, Smith L, Redfield C, Schwalbe H (2001) Chemical shifts in denatured proteins: resonance assignments for denatured ubiquitin and comparisons with other denatured proteins. J Biomol NMR 19:153–165
Roger B, Al-Bassam J, Dehmelt L, Milligan R, Halpain S (2004) MAP2c, but not tau, binds and bundles F-actin via its microtubule binding domain. Curr Biol 14:363–371
Rovnyak D, Frueh DP, Sastry M, Sun ZYJ, Stern AS, Hoch JC, Wagner G (2004) Accelerated acquisition of high resolution triple-resonance spectra using non-uniform sampling and maximum entropy reconstruction. J Magn Reson 170(1):15–21
Sattler M, Schleucher J, Griesinger C (1999) Heteronuclear multidimensional NMR experiments for the structure determination of proteins in solution employing pulsed field gradients. Prog Nucl Magn Reson Spectrosc 34(2):93–158
Schmieder P, Stern A, Wagner G, Hoch J (1994) Improved resolution in triple-resonance spectra by nonlinear sampling in the constant-time domain. J Biomol NMR 4:483–490
Shaka A, Barker P, Freeman R (1985) Computer-optimized decoupling scheme for wideband applications and low-level operation. J Magn Reson 64(3):547–552
Shaka A, Lee C, Pines A (1988) Iterative schemes for bilinear operators—application to spin decoupling. J Magn Reson 77(2):274–293

Stanek J, Koźmiński W (2010) Iterative algorithm of discrete Fourier transform for processing randomly sampled NMR data sets. J Biomol NMR 47:65–77

Stern A, Li K, Hoch J (2002) Modern spectrum analysis in multidimensional NMR spectroscopy: comparison of linear-prediction extrapolation and maximum-entropy reconstruction. J Am Chem Soc 124:1982–1993

Sun ZY, Frueh D, Selenko P, Hoch J, Wagner G (2005) Fast assignment of 15N-HSQC peaks using high-resolution 3D HNcocaNH experiments with non-uniform sampling. J Biomol NMR 33:43–50

Szyperski T, Wider G, Bushweller J, Wüthrich K (1993) Reduced dimensionality in triple-resonance NMR experiments. J Am Chem Soc 115:9307–9308

Tamiola K, Acar B, Mulder FA (2010) Sequence-specific random coil chemical shifts of intrinsically disordered proteins. J Am Chem Soc 132(51):18000–18003

Tompa P (2005) The interplay between structure and function in intrinsically unstructured proteins. FEBS Lett 579(15):3346–3354

Wen J, Wu J, Zhou P (2011) Sparsely sampled high-resolution 4-D experiments for efficient backbone resonance assignment of disordered proteins. J Magn Reson 209:94–100

Wille H, Mandelkow E, Mandelkow E (1992) The juvenile microtubule-associated protein MAP2c is a rod-like molecule that forms antiparallel dimers. J Biol Chem 267(15):10737–10742

Yao J, Chung J, Eliezer D, Wright PE, Dyson HJ (2001) NMR structural and dynamic characterization of the acid-unfolded state of apomyoglobin provides insights into the early events in protein folding. Biochemistry 40(12):3561–3571

Zamora-Leon SP, Lee G, Davies P, Shafit-Zagardo B (2001) Binding of Fyn to MAP-2c through an SH3 binding domain. Regulation of the interaction by ERK2. J Biol Chem 276(43):39950–39958

Zawadzka-Kazimierczuk A, Koźmiński W, Šanderová H, Krásný L (2012) High dimensional and high resolution pulse sequences for backbone resonance assignment of intrinsically disordered proteins. J Biomol NMR 52(4):329–337